THE JOURNAL OF BIOLOGICAL CHEMISTRY VOL. 283, NO. 34, pp. 23104–23112, August 22, 2008

On the Significance of Toc-GTPase Homodimers*

Received for publication, December 31, 2007, and in revised form, April 15, 2008 Published, JBC Papers in Press, June 8, 2008, DOI 10.1074/jbc.M710576200

Patrick Koenig[‡1], Mislav Oreb[§], Karsten Rippe[¶], Claudia Muhle-Goll[‖], Irmgard Sinning[‡], Enrico Schleiff[§], and Ivo Tews[‡2]

From the [‡]Heidelberg University Biochemistry Center, Im Neuenheimer Feld 328, 69120 Heidelberg, Germany, [§]JWGU Frankfurt am Main, Cluster of Excellence Macromolecular Complexes, Department of Biosciences, Max-von-Laue Strasse 9, 60439 Frankfurt, Germany, [¶]Deutsches Krebsforschungszentrum and BIOQUANT, Research Group Genome Organization and Function, Im Neuenheimer Feld 280, 69120 Heidelberg, Germany, and [‖]Karlsruhe Institute of Technology, Institut für Biologische Grenzflächen, POB 3640, 76021 Karlsruhe, Germany

Precursor protein translocation across the outer chloroplast membrane depends on the action of the Toc complex, containing GTPases as recognizing receptor components. The G domains of the GTPases are known to dimerize. In the dimeric conformation an arginine contacts the phosphate moieties of bound nucleotide in *trans*. Kinetic studies suggested that the arginine in itself does not act as an arginine finger of a reciprocal GTPase-activating protein (GAP). Here we investigate the specific function of the residue in two GTPase homologues. Arginine to alanine replacement variants have significantly reduced affinities for dimerization compared with wild-type GTPases. The amino acid exchange does not impact on the overall fold and nucleotide binding, as seen in the monomeric x-ray crystallographic structure of the *Arabidopsis* Toc33 arginine-alanine replacement variant at 2.0 Å. We probed the catalytic center with the transition state analogue GDP/AlF_x using NMR and analytical ultracentrifugation. AlF_x binding depends on the arginine, suggesting the residue can play a role in catalysis despite the non-GAP nature of the homodimer. Two non-exclusive functional models are discussed: 1) the coGAP hypothesis, in which an additional factor activates the GTPase in homodimeric form; and 2) the switch hypothesis, in which a protein, presumably the large Toc159 GTPase, exchanges with one of the homodimeric subunits, leading to activation.

The vast majority of GTPases serve as molecular switches that regulate various signaling and transport processes within the cell. GTPases bind and hydrolyze GTP and the nucleotide is recognized by five loops of specific function, called G1–G5 loop (1). Typically, GTPases have only low intrinsic GTPase rates and rely on auxiliary proteins such as GTPase activating proteins (GAPs)[3] and guanosine nucleotide exchange factors (2). Regulation of hydrolytic activity can in various ways also be achieved through dimerization of the GTPase. For the different studied cases of dimeric GTPases (3–8), differences exist with respect to interaction mode or the function of dimerization.

The small GTPases of the Toc34 type (9) and the multidomain GTPases of the Toc159 type (9, 10) are subunits of the membrane-inserted Toc complex which transports precursor proteins from the cytoplasm across the outer chloroplast envelope membrane (11–13). Although Toc GTPases can homo- and heterodimerize *in vitro* (14–23), mechanistic models of protein import consider a Toc34/Toc159 interaction (24). Previous three-dimensional structures show the *ps*Toc34 GTPase from *Pisum sativum* in the GDP (17) and in the GMPPNP (25)-bound states as dimers. The functional homologue *at*Toc33 from *Arabidopsis thaliana* (14, 26) is a monomer in both nucleotide loading states (16, 25). Both GTPases can homodimerize in solution (15, 16, 25), but *at*Toc33 has a lower association constant compared with *ps*Toc34 (16, 25, 27).

It is not entirely clear how dimerization and hydrolytic activity are linked (16, 18, 23, 25). This is surprising as the dimerization interface not only involves a number of Toc-specific insertions (17, 25) but also several G loops that bind the nucleotide. An arginine, contacting nucleotide in *trans* in dimeric GTPase complexes, has been assigned a function in dimer formation (15, 23), in nucleotide recognition (16), and in catalysis (16, 17, 23). To decipher the specific role of this residue, we studied the GTPases *ps*Toc34 and *at*Toc33 as well as arginine to alanine replacement variants *ps*Toc34^{R133A} and *at*Toc33^{R130A}. We discuss the physiological role of Toc GTPases Toc33/34 homodimers, which are in abundance in the Toc complex (28–30).

EXPERIMENTAL PROCEDURES

Cloning and Protein Purification—Mutants of *at*Toc33 and *ps*Toc34 were generated by PCR using *at*Toc33 (amino acids (aa) 1–251) (14) and *ps*Toc34 (aa 1–267) (25) as templates. Constructs were cloned into pET21d (Novagen, Madison, WI) to generate *at*Toc33^{R130A} and *ps*Toc34^{R133A} with C-terminal hexahistidine tag.

* The work was supported by Deutsche Forschungsgemeinschaft Grant SFB594-B11 (to E. S.) and by a grant from the Volkswagenstiftung (to E. S. and K. R.). The costs of publication of this article were defrayed in part by the payment of page charges. This article must therefore be hereby marked "*advertisement*" in accordance with 18 U.S.C. Section 1734 solely to indicate this fact.

The atomic coordinates and structure factors (code 3DEF) have been deposited in the Protein Data Bank, Research Collaboratory for Structural Bioinformatics, Rutgers University, New Brunswick, NJ (http://www.rcsb.org/).

[1] Supported by a fellowship of the interdisciplinary Ph.D. program "Molecular machines: mechanisms and functional interconnections" of the Land Baden-Württemberg (to I. S.).

[2] To whom correspondence should be addressed. Tel.: 49-6221-5447-85; Fax: 49-6221-5447-90; E-mail: ivo.tews@bzh.uni-heidelberg.de.

[3] The abbreviations used are: GAP, GTPase-activating protein; *at*, *A. thaliana*; *ps*, *P. sativum*; Toc/Tic, translocon at the outer/inner chloroplastic envelope membrane; HPLC, high performance liquid chromatography; GMPPNP, guanosine 5′-(β,γ-imido)triphosphate; c(s), continous distribution.

Recombinant proteins were purified using nickel affinity chromatography (GE Healthcare) in 50 mM Tris buffered at pH 7.4 containing 500 mM NaCl, 10 mM imidazole, 5 mM $MgCl_2$, 10% glycerol, and 0.7 mM β-mercaptoethanol as running buffer; elution buffer additionally contained 500 mM imidazole. For crystallization the protein was further purified by gel filtration using a Superdex 75 prep grade 26/60 column (GE Healthcare) with 20 mM HEPES buffered at pH 7.4 containing 150 mM KCl, 3 mM $MgCl_2$, and 0.7 mM β-mercaptoethanol as running buffer. For analytical ultracentrifugation, *ps*Toc34 and *ps*Toc34^{R133A} were further purified after nickel purification by size exclusion chromatography using a Superdex 75 26/60 column and 20 mM Tris buffer at pH 8.5 containing 100 mM NaCl and 3 mM $MgCl_2$. For nucleotide exchange of *ps*Toc34, buffer exchange after nickel affinity purification with 20 mM Tris at pH 8.5, containing 100 mM NaCl and 3 mM $MgCl_2$, was performed on a PD10 column (GE Healthcare). The protein was incubated with 2 mM GMPPNP and 100 units of alkaline phosphatase (New England Biolabs, Frankfurt, Germany) for 10 h at 15 °C. A subsequent purification step by nickel affinity chromatography and size exclusion chromatography was performed to remove alkaline phosphatase.

Crystallography—*at*Toc33^{R133A} was crystallized at a concentration of 0.8 mM using sitting drop vapor diffusion and a 2-μl drop size at 19 °C. Crystals were obtained within 3 days in 20% polyethylene glycol 3350 with 0.2 M NH_4Cl, subsequently frozen in liquid nitrogen, and stored using mother liquor containing an additional 20% glycerol as cryoprotectant. Data were collected at European Synchrotron Radiation Facility, Grenoble, France, on beamline ID14-4 at a wavelength of 0.933 Å on an ADSC Quantum-q4 CCD imaging device.

Data were integrated and scaled with the HKL software (31). Data reduction, Free-R assignment, and all further data manipulation were carried out with the CCP4 suite of programs (32). The structure was determined by molecular replacement using the program MOLREP (33) with *at*Toc33 as a search model (PDB code 3BB3 (25)). Iterative model building and refinement were carried out with the programs "coot" (34) and REFMAC5 (35) cycled with ARP (36) Data collection and refinement statistics are summarized in Table 1.

NMR Spectroscopy—^{19}F NMR spectra were measured on a DRX300 spectrometer (Bruker, Rheinstetten, Germany) operating at 270 MHz. The spectra were acquired at 25 °C using protein at a concentration of 0.5 mM in 20 mM Tris buffered at pH 7.0 containing 75 mM NaCl, 3 mM $MgCl_2$, 10 mM NaF, 1 mM $AlCl_3$, and 10% D_2O added before acquisition. The spectra were referenced to external trifluoracetate. A 90° pulse was used with a repetition rate of 2 s. 4096 free induction decays were summed up. The spectra were processed with TOPSPIN (Bruker, Germany).

Biochemical and Biophysical Assays—For analytical ultracentrifugation, nucleotide load of the protein sample was controlled by reverse phase HPLC as described (25). A preparation of GDP-loaded GTPase was split, and to one half of the preparation 10 mM NaF and 1 mM $AlCl_3$ were added. Both samples were incubated overnight at 4 °C. The final protein concentration for analytical ultracentrifugation on a Beckman Optima XL-A ultracentrifuge equipped with absorbance optics and an An60 Ti rotor (Beckman Coulter, Fullerton, CA) was adjusted to 45 μM. Sedimentation velocity runs were carried out at 20 °C at 40,000 rpm using the size exclusion buffer as described above as reference. Buffer density (1.00314 ml g^{-1}), buffer viscosity (1.002 millipascals·s) as well as the partial specific volume of *ps*Toc34 based on amino acid sequence ($\bar{v}$ = 0.7410 ml g^{-1}) were calculated using the program SEDNTERP, Version 1.05.[4] Sedimentation coefficients were determined from the c(s) distribution using the program SEDFIT (37, 38), normalized for water and 20 °C.

Dimerization behavior of nickel affinity purified *at*Toc33 and *at*Toc33^{R130A} was analyzed by size exclusion chromatography using a Superdex75 16/100 (GE Healthcare) equilibrated with 20 mM Tris buffered at pH 8.5 containing 75 mM NaCl and 3 mM $MgCl_2$. For molecular weight determination, 100 μl of nickel affinity-purified protein at a concentration of ~0.6 mM was loaded onto a Superdex75 HR 10/300 gel filtration column (GE Healthcare) equilibrated with 20 mM Tris buffered at pH 7 containing 75 mM NaCl and 3 mM $MgCl_2$. Alternatively, the buffer contained 10 mM NaF and 1 mM $AlCl_3$. For in-line detection, a Mini Dawn light scattering instrument (Wyatt Technology, Santa Barbara, CA) and a refractory index detector (WGE Dr. Bures, Dallgow, Germany) were used. Data were evaluated using the AstraV software (Wyatt Technology).

GTPase activities of *at*Toc33, *at*Toc33^{R130A}, *ps*Toc34, and *ps*Toc34^{R133A} were determined by a HPLC-based hydrolysis assay as described previously (25). Protein was used at a concentration of ~0.8 mM in 20 mM Tris-HCl buffered at pH 8.0 containing 75 mM KCl and 5 mM $MgCl_2$.

TABLE 1
Crystallographic analysis

	*at*Toc33^{R130A}·GDP
Space group	$P4_32_12$
Unit cell $a = b$, c (Å)	71.44, 112.46
Solvent content (%)	43
No. of mol (in the asymmetric unit)	1
Resolution (Å)	30.00-1.96
Average B (Å^2)	25
Unique reflections	21,984
Mosaicity (°)	0.92
R_{sym} (%)[a]	3.7
Completeness (%)	97.5
⟨I⟩/⟨sigI⟩	37.2
Redundancy	6.9
High resolution shell (Å)	1.99-1.96
High resolution shell R_{sym} (%)[a]	28.4
High resolution shell Completeness (%)	96.5
High resolution shell ⟨I⟩/⟨sigI⟩	4.4
Redundancy	6.2
Amino acids	2–68, 72–250
Total protein atoms (including double conformations)	2,175
Water	212
Ligand atoms	GDP, Mg^{2+}
Root mean square deviation bonds (Å)	0.017
Root mean square deviation angles (°)	1.598
R_{free} (%)[b]	24.07
R_{work} (%)[c]	19.60

[a] $R_{sym} = \Sigma_h\Sigma_i|I(h) - I(h)_i|/\Sigma_h\Sigma_i I(h)_i$, where $I(h)$ is the mean intensity.
[b] 5% of the data were excluded to calculate R_{free}.
[c] $R_{work} = \Sigma_h||F_{obs}(h)| - |F_{calc}(h)||/\Sigma h|F_{obs}(h)|$, where $F_{obs}(h)$ and $F_{calc}(h)$ are observed and calculated structure factors, respectively.

[4] From J. Philo, D. Hayes, and T. Laue.

RESULTS

Homodimerization and Nucleotide Recognition of Small Toc-GTPases—To understand the function of dimerization of the two homologous GTPases *at*Toc33 and *ps*Toc34, we first analyzed the previously published three-dimensional structures of *ps*Toc34 (17, 25). Five G loops bind the nucleotide, as in other GTPases (1), but in addition, the G loops G2, G3, and G4 are involved in dimerization (*gray*, *blue*, and *green* in Fig. 1*A*). Furthermore, the conserved box loop (CB loop) contributes to dimerization ((25) *red* in Fig. 1*A*). This sequence motif is unique to Toc and the so called Aig-like GTPases (39). Also at the dimer interface is helix α5 (*green* in Fig. 1*A*).

We investigated how nucleotide recognition and dimerization are linked, as the G loops are located at the interface. We note a change in function of the G4 loop which has lost properties of nucleotide recognition to gain properties in dimerization. Small Toc GTPases have a conserved histidine in the G4 loop (sequence motif THAQ) not present in the G4 loop of canonical small GTPases like the GTPase Ras p21 (sequence motif NK*X*D (17, 40, 41); Fig. 1*B*). In *ps*Toc34, *ps*His-163 of the G4 loop is in hydrogen-bonding distance to *ps*Tyr-132 in the CB loop of the homodimerization partner in *trans* (Fig. 1*C*). *ps*His-163 further makes a π-stacking interaction with the guanine ring of the base. The Toc34 G4 loop is deprived of a central aspartate residue that in small GTPases normally would specify the nucleotide through direct interaction with N1 and the 2-amino group of the guanine base (Fig. 1, *B–D*). Consequently, in *ps*Toc34 other interactions are responsible for nucleotide recognition; the G5, glutamate contacts guanosine N1 directly and the guanosine 2-amino group via one bridging water (*WAT*, Fig. 1*C*). The lack of specificity explains the reported hydrolysis of Xanthosine-5′-triphosphate (42, 43).

The Structural Impact of R130A Exchange on Nucleotide Recognition—The CB loop not only provides *ps*Tyr-132 but, more importantly, the two adjacent arginines, *ps*Arg-128 and *ps*Arg-133, for dimerization. Replacement of any of these arginines with alanine leads to abrogation of dimerization (15–17, 23). A structural study carried out at 3.2 Å resolution on *at*Toc33^{R130A} reported a monomeric structure of the GTPase (PDB code 2J3E (16)). Interestingly, the guanosine moiety was fitted in an unusual conformation in which the guanidine group was turned by 150° (16). Given the analysis presented above on incomplete nucleotide recognition by the G4/G5 loops, one might suppose that this unusual nucleotide conformation could occur, even though it would be in disagreement with other GTPase structures.

The earlier data prompted us to initiate a crystallographic study with the aim to collect atomic resolution data on *at*Toc33^{R130A}. The expression construct encoded amino acids 1–251 rather than amino acids 1–256 as in the previous study (16). Furthermore, crystallization conditions were slightly different; we used 20% polyethylene glycol 3350, 0.2 M NH_4Cl, pH 7.4, instead of 30% polyethylene glycol 4000, 0.2 M ammonium acetate, 0.05 M sodium acetate, pH 4.8 with added NADH (16). The crystals diffracted to a Bragg spacing below 2 Å using synchrotron light (Table 1). We determined the structure by molecular replacement using the model of native *at*Toc33 (PDB code 3BB3 (25)). Space group symmetry and molecular packing are identical to the earlier study on *at*Toc33^{R130A} (16) but different from wild-type *at*Toc33. At position 130, no side chain electron density is seen, consistent with the arginine-alanine exchange. All three structures are observed in the GDP-bound form and are highly similar (with respective root mean square deviation values of 0.58 Å over 231 C_α positions and of 1.1 Å over 233 C_α positions for comparison of *at*Toc33^{R130A} with native *at*Toc33 (PDB code 3BB3 (25) and with the earlier structure of *at*Toc33^{R130A} (PDB code 2J3E (16)). Importantly, structural changes reported to occur in *at*Toc33^{R130A} (16) are not confirmed.

Initial refinement without nucleotide resulted in clear negative $F_{obs} - F_{calc}$ density for the nucleotide, as shown in Fig. 2*A*. Compared with the earlier report (16), the *syn* conformation of the glycosidic bond in the GDP molecule is not confirmed (Fig. 2*A*, *white nucleotide*). Instead, the common anti-conformation is observed (Fig. 2*A*, *black nucleotide*). Thus, although it was previously suggested that a change in nucleotide conformation might have occurred either by lack of dimerization or as a result of the *at*R130A exchange (16), comparison with the wild-type structure and the high resolution structure of *at*Toc33^{R130A} presented here rule out this possibility, demonstrating that nucleotide binding is unaffected.

Effect of Arginine to Alanine Exchange on the Homodimerization of Toc34—In the structure of dimeric *ps*Toc34, an arginine (Arg-133, the equivalent of *at*Arg-130) contacts the β- and γ-phosphate groups *in trans*. This interaction is suggestive of a function as arginine finger often found in GAP-GTPase interactions (Fig. 1*C*) (44). This has led to the proposal that the *ps*Toc34 homodimer could be a self-activating GAP complex (16, 17). Furthermore, this interaction has been described to be pivotal for dimerization (15, 16, 23).

We established the dimerization properties of *at*Toc33 and of *at*Toc33^{R130A} using size exclusion chromatography (Fig. 2*B*). As the chromatogram shows, both proteins dimerize. However, the dimerization behavior of *at*Toc33^{R130A} is impaired. The difference in migration behavior of both, monomeric and dimeric species, can be explained by a presumed difference in dimerization behavior. A fast dimerization equilibrium in *at*Toc33 would lead to a decreased apparent size of the dimer; in turn, it would increase the apparent size of the monomer. This is supported by static light scattering data, given below. Although dimeric and monomeric species do not base-line separate for *at*Toc33, *at*Toc33^{R130A} is different and shows base-line separation.

Effect of Arginine to Alanine Exchange on the Hydrolysis Rate of Toc34—Previously, it was shown in multiple turnover assays that arginine-alanine replacement impacts on GTP hydrolysis. *at*Toc33^{R130A} shows a minor reduction in hydrolysis rate compared with *at*Toc33 (15, 16), and *ps*Toc34^{R133A} shows a loss of hydrolytic activity (23).

We investigated the effect of an arginine to alanine replacement on GTP hydrolysis using an HPLC-based single turnover assay for determination of enzymatic rates (45). The assay was carried out at higher concentrations than the multiple turnover experiments, allowing for dimer formation of wild-type proteins (see "Experimental Procedures" for details). *at*Toc33^{R130A}

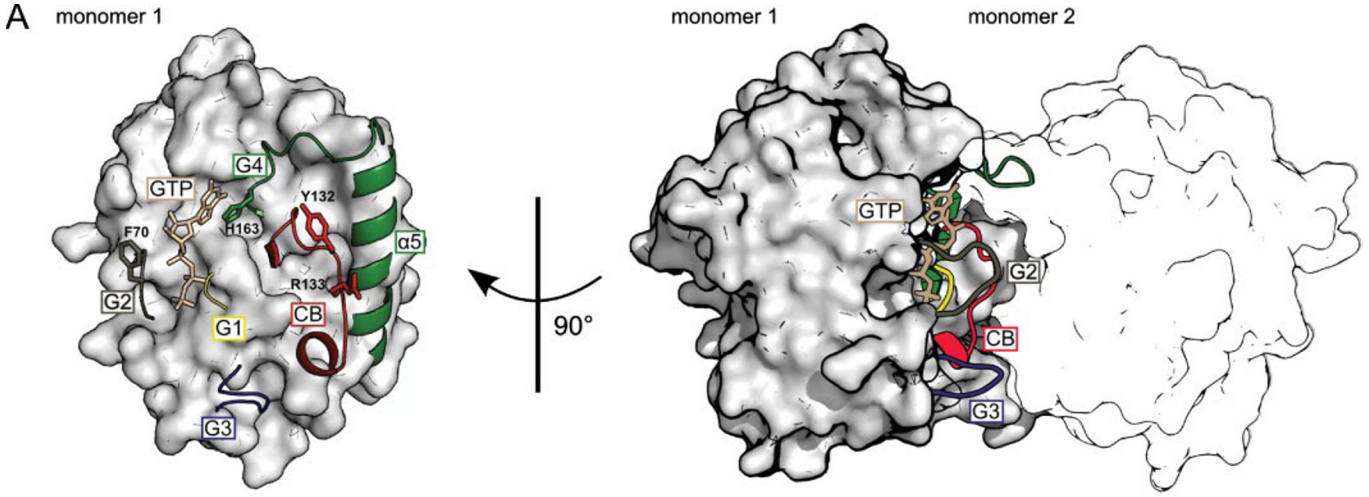

B

		G4	
atToc33	155	**L L V L T H A Q F S P P D**	167
atToc34	157	A L V L T H A Q F S P P D	169
Bnap1	155	L L V L T H A Q F S P P D	167
Mtru	158	I V A L T H A Q F S P P D	170
Oluc	191	V L G F S H A Q T T P T D	203
Otau	187	V L G F S H A Q T T P P D	199
Ovio	155	L L V L T H A Q F S P P D	167
Ppat1	156	V I V L T H A Q F S P S D	168
Ppat2	155	I V V F T H A E I H L E D	167
Ppat3	156	I I A L T H A Q L S P P D	168
psToc34	158	**I V A L T H A Q F S P P D**	170
Ptri1	155	L L V L T H A Q L C P P D	167
Ptri2	155	L L V L T H A Q L C P P D	167
Stub	156	L V V L T H A Q V S P P D	168
Vvin	156	V V V L T H A Q L S P P D	168
Zmay1	156	L V V L T H A Q L S P P D	168
Zmay2	156	L V V L T H A Q L S P P D	168
hsRas/p21	112	V L V G N K C D L A A R T	124

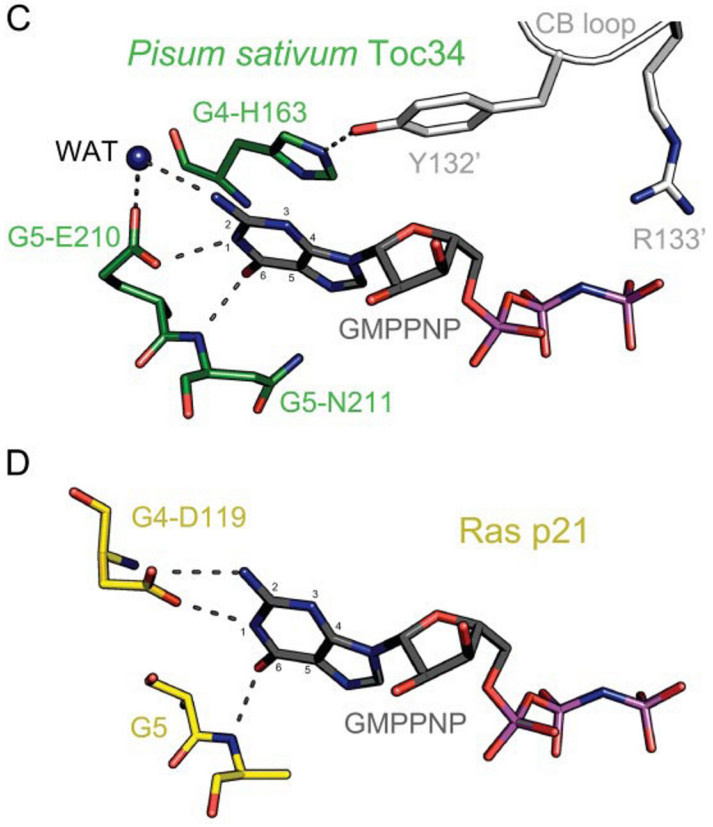

FIGURE 1. **Analysis of dimerization specific features of the GTPase *ps*Toc34 from *P. sativum* (GMMPNP bound state, PDB code 3BB4 (25)).** *A*, *left-hand side*, view onto the dimerization face of a single monomer; *right-hand side*, in the crystal structure, one monomer, in *gray*, interacts with a second monomer, in *white*. Between the two views, the gray monomer is turned by 90° around a vertical axis. The molecules are shown as surface representations; critical elements involved in dimerization are visualized in color (G2, *gray*; G3, *blue*; G4, *green*; CB loop, *red*). Residues discussed under "Results" are numbered and shown in *stick representation*. *B*, alignment of the G4 loop region of Toc34 GTPases with Ras p21, a representative of canonical small GTPases. Sequences used are: *atToc33*, *A. thaliana* Toc33 NP_171730; *atToc34*, *A. thaliana* Toc34 NP_196119; *Bnap1*, *Brassica napus* Toc33 AAQ17548; *Mtru*, *Medicago truncatula* Toc34 gb ABD28666.1; *Oluc*, *Ostreococcus lucimarinus* predicted small Toc GTPase CCE9901 XP_001417009.1; *Otau*, *Ostreococcus tauri* Toc34 emb CAL53037.1; *Ovio*, *Orychophragmus violaceus* Toc33-like protein gb AAM77647.1; *Ppat1*, *Physcomitrella patens* Toc34-1 gb AAS47580.1; *Ppat2*, *P. patens* Toc34-2 gb AAS47581.1; *Ppat3*, *P. patens* Toc34-3 gb AAS47582.1; *psToc34*, *P. sativum* Toc34 Q41009; *Ptri1*, *Populus trichocarpa* small Toc GTPase LG_XIV0229; *Ptri2*, *P. trichocarpa* small Toc GTPase LG_II1667; *Stub*, *Solanum tuberosum* GTP binding-like protein gb ABB16976.1; *Vvin*, *Vitis vinifera* hypothetical protein emb CAN63847.1; *Zmay1*, *Zea mays* Toc34-1 emb CAB65537.1; *Zmay2*, *Z. mays* Toc34-2 emb CAB77551.1; *hsRas/p21*, *H. sapiens* H-Ras p21 P01112. *C*, the G4 and G5 loops of *ps*Toc34 interact with the nucleotide. The 2-amido group of the nucleotide is only in indirect contact with the protein via a water molecule (*WAT*). Thus, guanosine and xanthosine nucleotides cannot be distinguished. *ps*His-163 makes a hydrogen-bonding contact with *ps*Tyr132′ of the CB loop of the interacting homodimerization partner. Also shown is *ps*Arg-133′, interacting with phosphate moieties of the dimerization partner. *D*, a similar representation as in *C* for the Ras p21 protein (GMMPNP-bound state, PDB code 5p21, (54)). The conserved Asp-119 in the G4 loop recognizes GTP specifically by interacting with N1 and the 2-amino group.

showed 0.6-fold hydrolytic activity compared with wild-type protein ($k_{cat} = (2.3 \pm 0.4) \times 10^{-5}$ s^{-1} for *at*Toc33^{R130A} and $k_{cat} = (4.4 \pm 0.7) \times 10^{-5}) \times 10^{-5}$ s^{-1} for wild-type *at*Toc33). Similarly, *ps*Toc34^{R133A} showed 0.3-fold hydrolytic activity of the wild-type GTPase ($k_{cat} = (1.9 \pm 0.7) \times 10^{-5}$ s^{-1} for *ps*Toc34^{R133A} and $k_{cat} = (8.4 \pm 0.7) \times 10^{-5}$ s^{-1} for wild-type

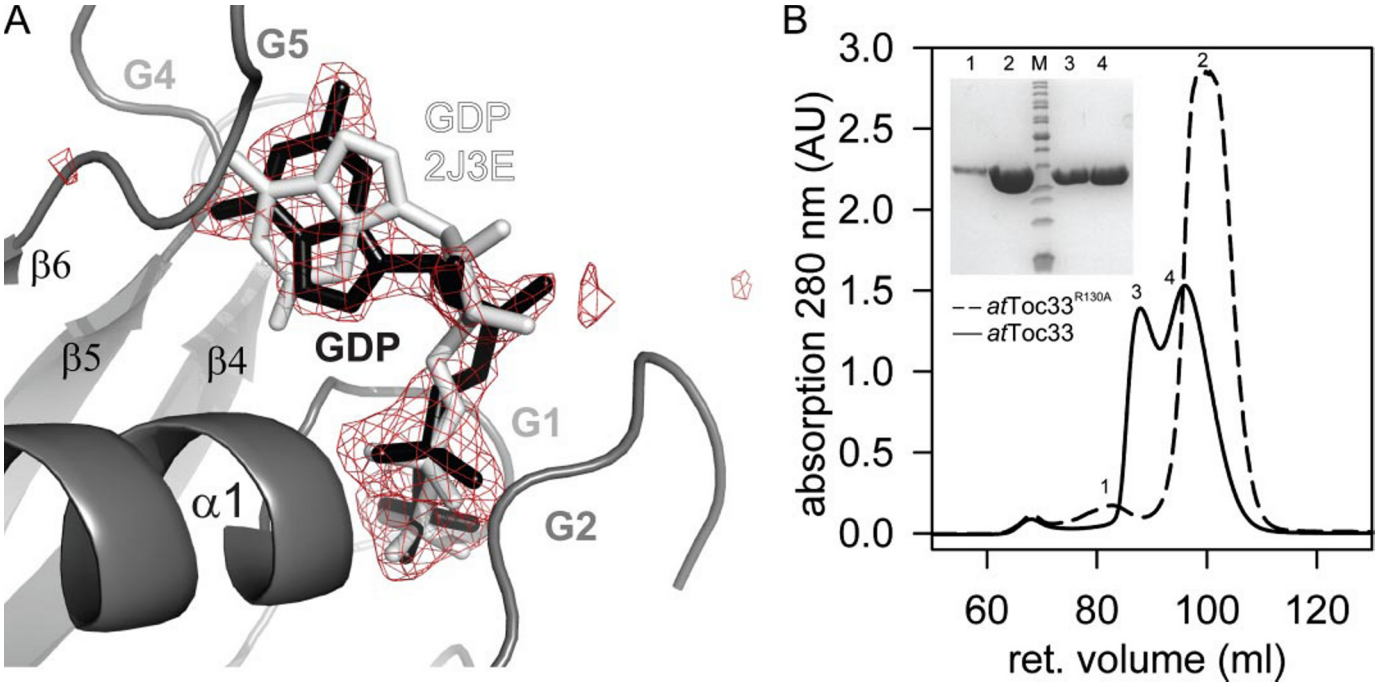

FIGURE 2. *A*, conformation of GDP in the *at*Toc33^{R130A} structure, with the GDP molecule shown in *black*. Difference density ($F_{obs} - F_{calc}$) obtained after structure refinement without nucleotide is shown as a *red* mesh. The final model includes nucleotide as shown in *black* (PDB code 3DEF); an altered GDP conformation was described previously (*white*, GDP molecule, PDB code 2J3E (16)). *B*, size exclusion chromatography of *at*Toc33 (*solid line*) and *at*Toc33^{R130A} (*dashed line*) using a Superdex75 16/100 column. Peak fractions were analyzed by SDS-PAGE (*inset*, molecular mass marker (*M*); from *top* to *bottom*: 200, 150, 120, 100, 85, 70, 60, 50, 40, 30, 25, 20, 15 and 10 kDa). *AU*, absorbance units.

protein). On one hand this establishes that *ps*Toc34^{R133A} possesses hydrolytic activity; on the other hand it demonstrates that the arginine-alanine exchange is only of minor influence on GTP hydrolysis in either GTPase. Apparent differences in determined hydrolysis rates with earlier reports (23) are likely explained by the different experimental setup of single and multiple turnover measurements.

Binding of AlF_x to psToc34—Because exchange of *at*Arg-130/*ps*Arg-133 with alanine has only limited influence on the GTP hydrolysis rate, we tested whether the respective arginines can act at all as arginine fingers, employing aluminum fluoride as a probe. Aluminum fluoride exists in an equilibrium of different species in solution and is, thus, abbreviated here as AlF_x. AlF_x can act as a transition state mimicry of phosphoryl transfer reactions (46) and has been shown to directly bind to the Gα proteins (47) that contain an intrinsic domain for stimulation of catalysis. Intrinsic stimulatory domains are absent in small GTPases such as Ras or Toc34, and they instead require a GAP for activation. For example AlF_x binding to Ras_{GDP} depends on the presence of the RasGAP proteins (48). GTPase·GAP·AlF_x complexes show AlF_x binding in the active site in place of the γ-phosphate and require GDP-loaded GTPase subunits. The GAP arginine finger is often present as binding partner. If *ps*Arg-133 acts as an arginine finger in the *ps*Toc34 dimer, AlF_x binding to *ps*Toc34 can be expected.

AlF_x binding to *ps*Toc34 was tested using ^{19}F NMR. A buffer solution containing $AlCl_3$ and NaF shows peaks at −77.0 ppm and at −41.7 ppm, corresponding to AlF_x and free F^- (Fig. 3*A*). After the addition of $psToc34_{GDP}$, a peak shifted by −24.5 ppm from the resonance signal of free F^- is observed at −66.2 ppm (Fig. 3*D*). The chemical shift, varying between −20 ppm and −22.4 ppm in previous studies (47, 49, 50), is indicative of AlF_x binding to nucleotide binding proteins and has been described before for *ps*Toc34 (17). To verify the specificity of the interaction in the catalytic center, *ps*Toc34 loaded with non-hydrolyzable GTP analogue GMPPNP was used. Because the binding site is occupied by the γ-phosphate of GMPPNP, specific binding of AlF_x to the γ-phosphate site can be excluded. Indeed, no binding of AlF_x is detected when the GMPPNP-loaded GTPase is investigated (Fig. 3*E*).

Effect of AlF_x on psToc34 Dimerization—We next tested the stability of the *ps*Toc34·GDP·AlF_x complex. Size exclusion chromatography of $psToc34_{GDP}$ in the presence of AlF_x in the buffer indicated stabilization of the dimer, as evidenced by a shift to a higher molecular weight species (data not shown). To quantify AlF_x-induced oligomerization, analytical ultracentrifugation was employed. Two samples were compared, distinguished by the presence of AlF_x. Without AlF_x treatment, *ps*Toc34 is present in monomer-dimer equilibrium (Fig. 4*A* (23, 25)). With AlF_x treatment, *ps*Toc34 was exclusively dimeric (Fig. 4*A*). Thus, the addition of AlF_x leads to stabilization of the *ps*Toc34 homodimer as reported for classical GTPase-GAP interactions like Ras-RasGAP (48).

When analytical ultracentrifugation was repeated with *ps*Toc34^{R133A}, no dimeric species was observed regardless of AlF_x treatment (Fig. 4*B*). This demonstrates that the effects seen before with wild-type *ps*Toc34 are specific and require the presence of *ps*Arg-133, in line with the NMR data (Fig. 3).

Influence of AlF_x on the Dimerization of atToc33—We then assayed the effect of AlF_x binding on the dimerization behavior of *at*Toc33. Because the protein exhibits a lower K_a for dimerization, analytical ultracentrifugation is impractical due to the

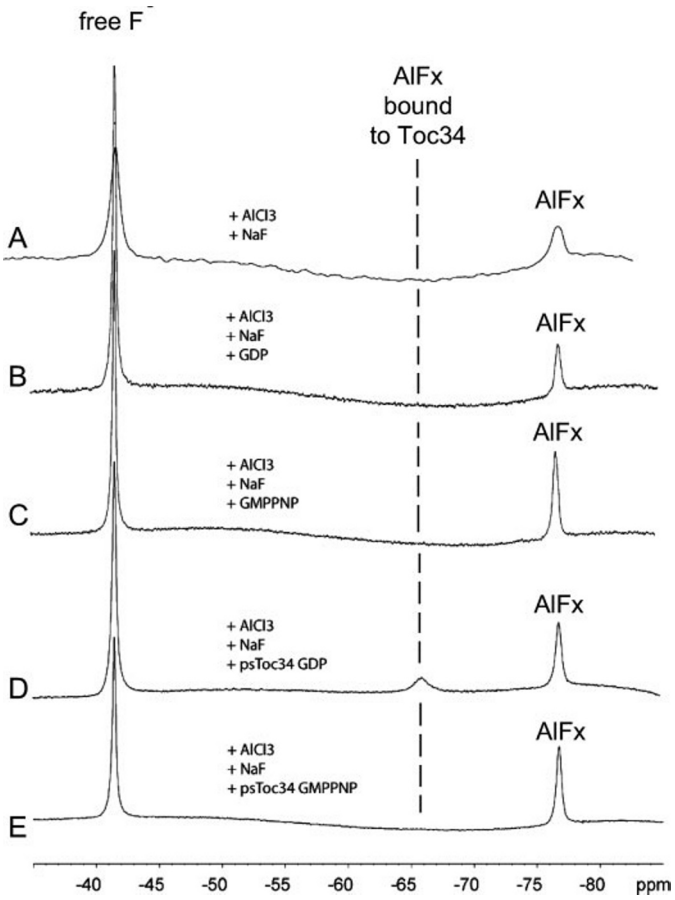

FIGURE 3. **Binding of AlF_x to *ps*Toc34 monitored by ^{19}F NMR.** *A*, ^{19}F NMR spectrum of buffer containing $AlCl_3$ and NaF shows two peaks (−77.0 ppm and −41.7 ppm) that have been assigned to free F^- and to AlF_x. *B* and *C*, the addition of nucleotides (GDP, GMPPNP) shows no changes in the spectrum compared with *A*. *D* upon addition of $psToc34_{GDP}$ to buffer containing $AlCl_3$ and NaF, an additional peak is observed at −66.2 ppm. *E* upon addition of $psToc34_{GMPPNP}$ to buffer containing $AlCl_3$ and NaF, no changes are observed in the spectrum compared with *A*.

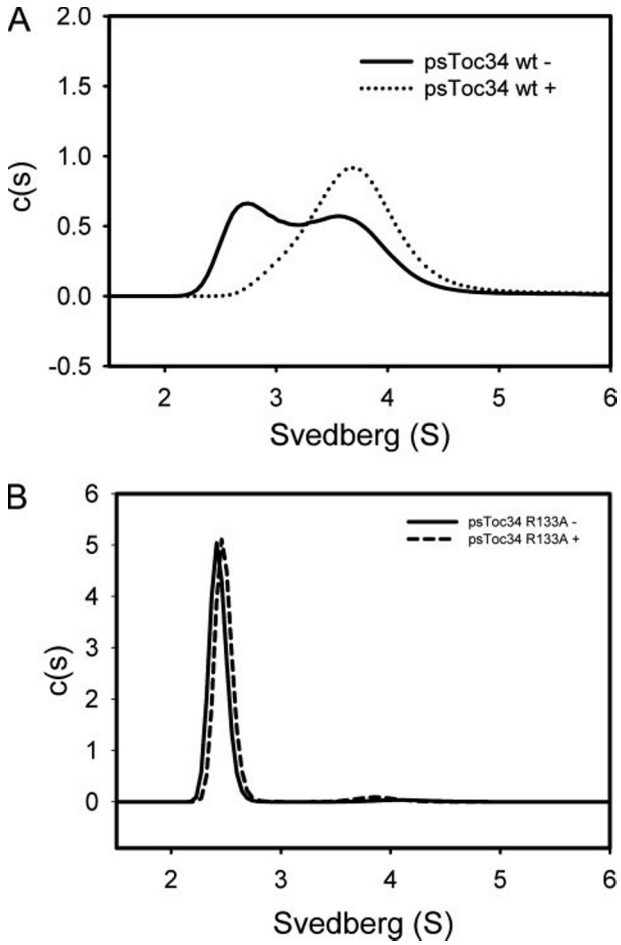

FIGURE 4. **Analysis of dimerization properties of *ps*Toc34 by analytical ultracentrifugation in the presence (*dashed line*) and absence of AlF_x (*solid line*).** The c(s) sedimentation coefficient distribution is shown. *A*, wild-type *ps*Toc34 protein with peaks at 2.7 S, corresponding to the monomeric protein species, and at 3.6 S, corresponding to the dimeric protein species. *B*, $psToc34^{R133A}$ with a single peak at 2.4 S, corresponding to the monomeric protein species.

high protein concentrations that would be required. Instead, we employed a setup where size exclusion chromatography was coupled with static light scattering and a refractive index detector to determine absolute molecular weights. This method does not require use of internal standards (51).

Similar to previous reports (15–17, 23), two molecular species were observed for wild-type *at*Toc33 in the absence of AlF_x (Fig. 5*A*). The analysis of static light scattering gave a signal yielding a molecular mass of 63 kDa for protein fractions in the first peak, which fits well with the value of 60 kDa for an *at*Toc33 dimer. However, protein fractions of the second peak displayed a molecular mass of 45 kDa; the tail of this second peak was fitted with a molecular mass of 36 kDa, likely to represent the monomer. The 45-kDa species likely results from a dynamic equilibrium between dimeric and monomeric species. Thus, *at*Toc33 exists as a fast equilibrium between the two states (compare Fig. 2*B*). This is consistent with data on *ps*Toc34 (23). When $atToc33^{R130A}$ was investigated, a single peak fitted to a molecular mass of 30–31 kDa was obtained, corresponding to monomeric protein (Fig. 5*B*).

When AlF_x was present in the buffer (Fig. 5*C*), *at*Toc33 shifted to a higher molecular mass species. Light scattering data were fitted to a molecular mass of 66 kDa, corresponding to the molecular mass of dimeric *at*Toc33 (60 kDa). Thus, stabilization of the dimeric species occurs with *at*Toc33 upon the addition of AlF_x. However the addition of AlF_x does not affect $atToc33^{R130A}$, which remains monomeric in the presence of AlF_x (Fig. 5*D*). The fit of the light scattering data yielded a molecular mass of 25 kDa.

The dimerization behavior of *at*Toc33 (Fig. 5*A*) and of *ps*Toc34 (Fig. 4*A*) are similar. The dimeric state of both proteins is stabilized by AlF_x (Figs. 4*A* and 5, *A* and *C*). With the arginine-alanine exchange mutants, it can be shown that binding is specific, since stabilization of the dimer requires the presence of *at*Arg-130/*ps*Arg-133 (Figs. 4*B* and 5, *B* and *D*).

DISCUSSION

Dimerization of Toc GTPases is generally assumed to be a feature of the assembly of the Toc apparatus (24). GTPase dimerization is recurrent, and the Toc GTPases are not exceptional in this respect. Documented examples of dimeric GTPases are, for instance, the SRP GTPases FtsY, Ffh (4, 5), and FlhF (3), the GTPases of the dynamin type, *e.g.* hGBP (7), the

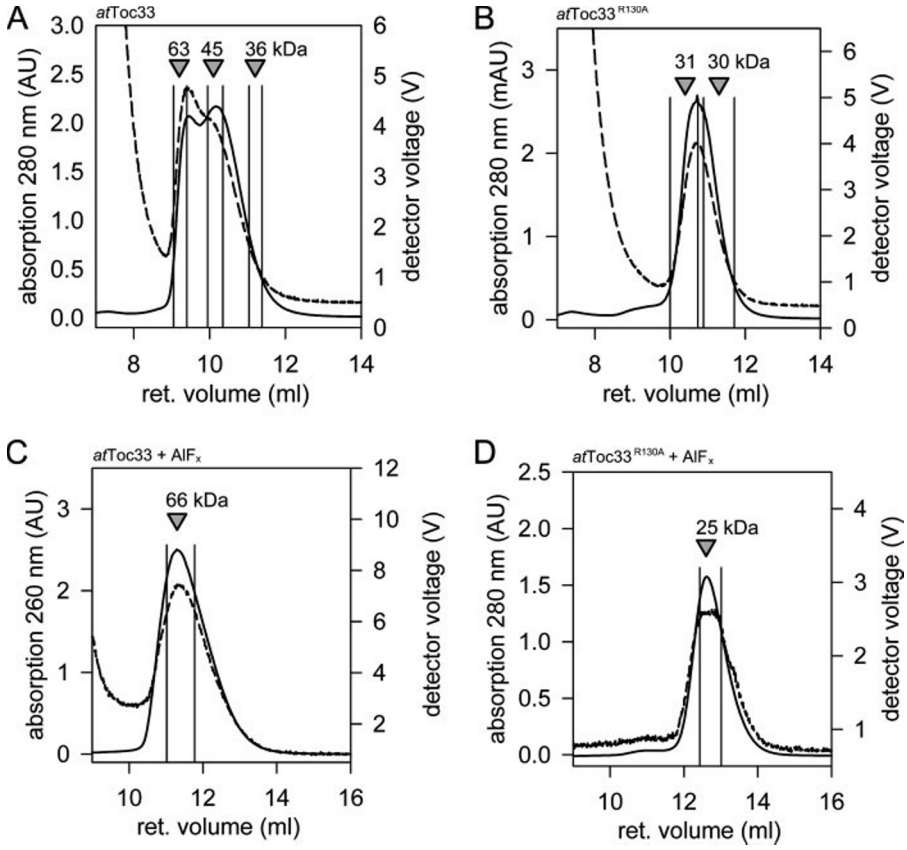

FIGURE 5. **Effect of AlF_x on the homodimerization of *at*Toc33 using size exclusion chromatography on a Superdex75 HR 10/300 column with UV detection (*dashed line*, *left-hand scale*) and in-line static light scattering (*solid line*, *right-hand scale*).** Areas averaged for size determination are indicated by *vertical lines* and annotated with the fitted molecular masses, as indicated by the *gray triangle*. *A*, *at*Toc33. *B*, *at*Toc33^{R130A}. *C*, *at*Toc33 in the presence of AlF_x. *D*, *at*Toc33^{R130A} in the presence of AlF_x. *AU*, absorbance units.

native PAGE, analytical ultracentrifugation, and size exclusion (15, 16, 23). It was shown that *at*Toc33^{R130A} and *ps*Toc34^{R133A} are unable to dimerize. In contrast, we show that *at*Toc33^{R130A} forms dimers at high protein concentrations using size exclusion chromatography (Fig. 2*B*). This suggests that Arg-130 in *at*Toc33 is a key, but not the sole player in homodimerization.

A function of *ps*Arg-133/*at*Arg-130 in nucleotide recognition was suggested on the basis of the previous 3.2 Å structure of *at*Toc33^{R130A} (16) in a monomeric state with an unusual nucleotide conformation. However, the limited resolution and the lack of a wild-type reference GTPase structure did not allow concluding whether the amino acid exchange directly affected the structure or whether the effect was indirect and caused by the lack of dimerization. Based on the 2-Å resolution structure presented here, an altered nucleotide conformation can be excluded. This is also evident from superposition with the now available monomeric wild-type *at*Toc33 structure (25).

Finally, participation of *ps*Arg-133 in catalysis was previously proposed on the basis of the crystal structure of *ps*Toc34 that showed this residue in a conformation similar to the classic GAP arginine finger (17). The transition state mimic GDP/AlF_x binds to the *ps*Toc34 homodimer but not to the *ps*Arg-133 mutant or to the GMPPNP-loaded GTPase (Fig. 3). This implies that AlF_x indeed acts as a transition state mimicry, demonstrating the arginine is in an appropriate conformation to act during catalysis. AlF_x binding also stabilizes the homodimers in *ps*Toc34 (Fig. 4*A*) and in *at*Toc33 (Fig. 5*C*). AlF_x-induced dimerization suggests a composite binding site formed by both dimerization partners involving *ps*Arg-133/*at*Arg-130.

Summing up from our studies on *ps*Arg-133/*at*Arg-130 and the literature, the following evidences doubt or directly contradict that small Toc GTPases form self-associating GAP-complexes (17). (i) Although it would be expected that a GAP complex favors the GTP state, it is observed that GMPPNP and GDP-loaded states of the GTPase both dimerize with similar efficiency (17, 25). (ii) Despite the stabilization of G loops in the dimerization interface, switch I retains some flexibility, which would be unexpected for a GAP complex (25). (iii) Despite the presence of the stabilizing arginine, reminiscent of the classic GAP arginine finger, the catalytic center is incomplete, as no residue for the positioning of the catalytic water is present (25); instead the catalytic site is accessible for solvent by a short tunnel. (iv) Kinetic data argue against the formation of a GAP-like

GTPase MnmE involved in tRNA modification (8), and the metal binding GTPase HypB (6). However, the dimerization interface is different between these GTPases, and so is the functional significance of dimerization of these various GTPases.

The isolated G domains of *ps*Toc34 and *at*Toc33 both dimerize, but they differ with respect to their dimerization properties (16, 25). The K_d of the *at*Toc33 dimer is about 1 order of magnitude higher than that for *ps*Toc34. Both K_d values are in the submillimolar range (25, 27). Although these figures, determined for the isolated GTPase, seem high, dimerization may still occur in the physiological context on the membrane or within the Toc complex via elevated local concentrations. Interaction may be helped by the C-terminal membrane anchor, not present in the proteins analyzed here.

The dimerization interface itself is preserved between different Toc34 GTPases (16) and involves the CB motif (25) as well as the G4/G5 loops, with G4 performing a dual role in nucleotide recognition and dimerization (Fig. 1*C*). The CB motif carries the arginine that contacts the nucleotide in *trans*, the function of which is controversially discussed with respect to dimerization, nucleotide binding, and catalysis (15–17, 23, 25). The function of this arginine, thus, requires further clarification, as it is the key to elucidate the task of the Toc34 homodimer.

The role of *ps*Arg-133/*at*Arg-130 in dimerization was previously investigated using a variety of techniques, including

complex; the acceleration of hydrolysis in GTPase·GAP complexes is typically in the order of 2–5 magnitudes (44). However, no significant catalytic activation is observed by dimer formation (23, 25). This is supported by data from arginine-alanine exchange proteins which show that replacement of *ps*Arg-133/*at*Arg-130 has only a minor effect on the hydrolysis rates of *ps*Toc34/*at*Toc33.

Thus, small Toc GTPases represent a paradox since *ps*Arg-133/*at*Arg-130 seems poised properly to act as an arginine finger, similar to that of a GAP, but hydrolysis rates are not accelerated. Acceleration of hydrolysis in Ras-like GTPases and their respective GAPs is mainly due to the positioning of a catalytic residue to polarize a water for hydrolytic attack (52). For instance, replacement of this crucial residue in a Ras:RasGAP system leads to abrogation of hydrolysis even when an arginine finger interaction is present (53). Our structural analysis of the Toc34 homodimer shows that despite the presence of *ps*Arg-133 or *at*Arg-130 the catalytic machinery remains incomplete, and an essential catalytic residue for the positioning of the catalytic water is required, explaining the minor effect of dimerization on hydrolysis rates (25).

We have previously shown that the nucleotide binding pocket is accessible in the $ps\text{Toc34}_{GMPPNP}$ homodimer and suggested a catalytic residue could be inserted into the catalytic center. This would functionally define the homodimer as a coGAP complex that requires both the homodimeric interaction and a third protein (coGAP hypothesis) (25). In addition, the third protein may also be required to stabilize and organize the catalytic center, then giving it its true GTPase/GAP type character. *ps*Arg-133/*at*Arg-130, thus, would fulfill the role of an arginine finger in catalysis only if the coGAP is present.

In a second proposal, the homodimer has to dissociate to become functional in the physiological context (switch hypothesis). Catalytic data suggest that the monomeric species requires interaction with another protein for activation. The large GTPase Toc159 is an obvious candidate for this interaction. Toc159 can supply an arginine, similar to what is seen in the homodimer but probably with slightly different geometry (25). The heterodimer is, thus, not only asymmetric but also different from the homodimer.

We conclude there may well be a physiological role for the small Toc33/34 GTPase homodimer, complementing the postulated heterodimer of small and large Toc GTPases. This is further supported by the stoichiometry of the Toc complex, where small GTPase subunits are in molar excess over large GTPase subunits. Hence, two differentially regulated events in the Toc-mediated chloroplast protein import cycle would exist.

Acknowledgments—We thank Anja Höfle and Broder Schmidt for experimental support and Jens Radzimanowski, Klemens Wild, and the staff at the European Synchrotron Radiation Facility synchrotron for help with data collection.

REFERENCES

1. Sprang, S. R. (1997) *Annu. Rev. Biochem.* **66,** 639–678
2. Vetter, I. R., and Wittinghofer, A. (2001) *Science* **294,** 1299–1304
3. Bange, G., Petzold, G., Wild, K., Parlitz, R. O., and Sinning, I. (2007) *Proc. Natl. Acad. Sci. U. S. A.* **104,** 13621–13625
4. Egea, P. F., Shan, S. O., Napetschnig, J., Savage, D. F., Walter, P., and Stroud, R. M. (2004) *Nature* **427,** 215–221
5. Focia, P. J., Shepotinovskaya, I. V., Seidler, J. A., and Freymann, D. M. (2004) *Science* **303,** 373–377
6. Gasper, R., Scrima, A., and Wittinghofer, A. (2006) *J. Biol. Chem.* **281,** 27492–27502
7. Prakash, B., Praefcke, G. J., Renault, L., Wittinghofer, A., and Herrmann, C. (2000) *Nature* **403,** 567–571
8. Scrima, A., and Wittinghofer, A. (2006) *EMBO J.* **25,** 2940–2951
9. Kessler, F., Blobel, G., Patel, H. A., and Schnell, D. (1994) *Science* **266,** 1035–1039
10. Chen, K., Chen, X., and Schnell, D. J. (2000) *Plant Physiol.* **122,** 813–822
11. Jarvis, P., and Robinson, C. (2004) *Curr. Biol.* **14,** 1064–1077
12. Kessler, F., and Schnell, D. J. (2004) *Trends Cell Biol.* **14,** 334–338
13. Soll, J., and Schleiff, E. (2004) *Nat. Rev. Mol. Cell Biol.* **5,** 198–208
14. Jelic, M., Soll, J., and Schleiff, E. (2003) *Biochemistry* **42,** 5906–5916
15. Weibel, P., Hiltbrunner, A., Brand, L., and Kessler, F. (2003) *J. Biol. Chem.* **278,** 37321–37329
16. Yeh, Y. H., Kesavulu, M. M., Li, H. M., Wu, S. Z., Sun, Y. J., Konozy, E. H., and Hsiao, C. D. (2007) *J. Biol. Chem.* **282,** 13845–13853
17. Sun, Y. J., Forouhar, F., Li Hm, H. M., Tu, S. L., Yeh, Y. H., Kao, S., Shr, H. L., Chou, C. C., Chen, C., and Hsiao, C. D. (2002) *Nat. Struct. Biol.* **9,** 95–100
18. Becker, T., Jelic, M., Vojta, A., Radunz, A., Soll, J., and Schleiff, E. (2004) *EMBO J.* **23,** 520–530
19. Smith, M. D., Hiltbrunner, A., Kessler, F., and Schnell, D. J. (2002) *J. Cell Biol.* **159,** 833–843
20. Wallas, T. R., Smith, M. D., Sanchez-Nieto, S., and Schnell, D. J. (2003) *J. Biol. Chem.* **278,** 44289–44297
21. Hiltbrunner, A., Bauer, J., Vidi, P. A., Infanger, S., Weibel, P., Hohwy, M., and Kessler, F. (2001) *J. Cell Biol.* **154,** 309–316
22. Ivanova, Y., Smith, M. D., Chen, K., and Schnell, D. J. (2004) *Mol. Biol. Cell* **15,** 3379–3392
23. Reddick, L. E., Vaughn, M. D., Wright, S. J., Campbell, I. M., and Bruce, B. D. (2007) *J. Biol. Chem.* **282,** 11410–11426
24. Oreb, M., Tews, I., and Schleiff, E. (2008) *Trends Cell Biol.* **18,** 19–27
25. Koenig, P., Oreb, M., Höfle, A., Kaltofen, S., Rippe, K., Sinning, I., Schleiff, E., and Tews, I. (2008) *Structure* **16,** 585–596
26. Jarvis, P., Chen, L. J., Li, H., Peto, C. A., Fankhauser, C., and Chory, J. (1998) *Science* **282,** 100–103
27. Oreb, M., Höfle, A., Mirus, O., and Schleiff, E. (2008) *J. Exp. Bot.* **59,** 2309–2316
28. Schleiff, E., Soll, J., Kuchler, M., Kuhlbrandt, W., and Harrer, R. (2003) *J. Cell Biol.* **160,** 541–551
29. Kikuchi, S., Hirohashi, T., and Nakai, M. (2006) *Plant Cell Physiol.* **47,** 363–371
30. Vojta, A., Alavi, M., Becker, T., Hormann, F., Kuchler, M., Soll, J., Thomson, R., and Schleiff, E. (2004) *J. Biol. Chem.* **279,** 21401–21405
31. Otwinowski, Z., and Minor, W. (1997) *Methods Enzymol.* **276,** 307–326
32. Collaborative Computational Project, N. (1994) *Acta Crystallogr. D Biol. Crystallogr.* **50,** 760–763
33. Vagin, A. A., and Teplyakov, A. (1997) *J. Appl. Crystallogr.* **30,** 1022–1025
34. Emsley, P., and Cowtan, K. (2004) *Acta Crystallogr. D Biol. Crystallogr.* **60,** 2126–2132
35. Murshudov, G. N., Vagin, A. A., and Dodson, E. J. (1997) *Acta Crystallogr. D Biol. Crystallogr.* **53,** 240–255
36. Lamzin, V. S., and Wilson, K. S. (1997) *Methods Enzymol.* **277,** 269–305
37. Dam, J., and Schuck, P. (2004) *Methods Enzymol.* **384,** 185–212
38. Schuck, P. (2000) *Biophys. J.* **78,** 1606–1619
39. Nitta, T., and Takahama, Y. (2007) *Trends Immunol.* **28,** 58–65
40. Bourne, H. R., Sanders, D. A., and McCormick, F. (1991) *Nature* **349,** 117–127
41. Leipe, D. D., Wolf, Y. I., Koonin, E. V., and Aravind, L. (2002) *J. Mol. Biol.* **317,** 41–72
42. Jelic, M., Sveshnikova, N., Motzkus, M., Horth, P., Soll, J., and Schleiff, E. (2002) *Biol. Chem.* **383,** 1875–1883
43. Aronsson, H., Combe, J., and Jarvis, P. (2003) *FEBS Lett.* **544,** 79–85

44. Scheffzek, K., and Ahmadian, M. R. (2005) *Cell. Mol. Life Sci.* **62,** 3014–3038
45. Hemsath, L., and Ahmadian, M. R. (2005) *Methods* **37,** 173–182
46. Wittinghofer, A. (1997) *Curr. Biol.* **7,** 682–685
47. Higashijima, T., Graziano, M. P., Suga, H., Kainosho, M., and Gilman, A. G. (1991) *J. Biol. Chem.* **266,** 3396–3401
48. Ahmadian, M. R., Mittal, R., Hall, A., and Wittinghofer, A. (1997) *FEBS Lett.* **408,** 315–318
49. Maruta, S., Henry, G. D., Sykes, B. D., and Ikebe, M. (1993) *J. Biol. Chem.* **268,** 7093–7100
50. Praefcke, G. J., Geyer, M., Schwemmle, M., Robert Kalbitzer, H., and Herrmann, C. (1999) *J. Mol. Biol.* **292,** 321–332
51. Margarit, S. M., Sondermann, H., Hall, B. E., Nagar, B., Hoelz, A., Pirruccello, M., Bar-Sagi, D., and Kuriyan, J. (2003) *Cell* **112,** 685–695
52. Scrima, A., Thomas, C., Deaconescu, D., and Wittinghofer, A. (2008) *EMBO J.* **27,** 1145–1153
53. Bollag, G., and McCormick, F. (1991) *Nature* **351,** 576–579
54. Pai, E. F., Krengel, U., Petsko, G. A., Goody, R. S., Kabsch, W., and Wittinghofer, A. (1990) *EMBO J.* **9,** 2351–2359